Sumitomo Drive Technologies

IDENTIFYING DEFECTIVE CYCLOIDAL REDUCTION COMPONENTS USING

VIBRATION ANALYSIS AND TECHNIQUES

VIRGIL COCHRAN

TODD BOBAK

US.SUMITOMODRIVE.COM

08FTM02

American Gear Manufacturers Association

Technical Resources

AGMA Technical Paper

A Methodology for Identifying Defective Cycloidal Reduction Components Using Vibration Analysis and Techniques

By V. Cochran and T. Bobak,
Sumitomo Drive Technologies

A Methodology for Identifying Defective Cycloidal Reduction Components Using Vibration Analysis and Techniques

Virgil Cochran and Todd Bobak, Sumitomo Drive Technologies

[The statements and opinions contained herein are those of the author and should not be construed as an official action or opinion of the American Gear Manufacturers Association.]

Abstract

For several years predictive maintenance has been gaining popularity as a method for preventing costly and time-consuming machine breakdowns. Vibration analysis is the cornerstone of predictive maintenance programs, and the equations for calculating expected vibration frequencies for bearings and toothed gear sets are widely available. Cycloidal reducers present a special case due to the nature of their reduction mechanism. This paper will describe a method for utilizing vibration analysis in order to identify a defective cycloidal ring gear housing, disc, and eccentric bearing.

American Gear Manufacturers Association
500 Montgomery Street, Suite 350
Alexandria, Virginia, 22314

October, 2008

ISBN: 978-1-55589-932-5

A Methodology for Identifying Defective Cycloidal Reduction Components Using Vibration Analysis and Techniques

Virgil Cochran and Todd Bobak, Sumitomo Drive Technologies

Introduction

Predictive maintenance is becoming a popular method for preventing costly and time–consuming equipment failure. It's applied most often to assembly lines, where the unexpected failure of a critical machine can lead to thousands of lost dollars per hour of downtime. Predictive maintenance via vibration analysis can indicate, before failure occurs, whether internal machine components are worn and require replacement. The advanced notification that predictive maintenance provides allows users to repair their machines during scheduled downtime, thereby preventing unexpected failures during production hours. The benefits are maintenance and spare parts cost reductions along with increases in production time. Product quality increases are also realized since machines can be maintained in good condition consistently (1).

Some vibration analysis software packages include bearing frequency and gear mesh information in their databases, and by entering system information the software provides the user with the operating frequencies of interest.

Cycloidal reducers, however, are more complex than toothed gear systems. They contain more rolling components than toothed gear sets, which makes calculating the expected operating frequencies difficult, see figure 1. However, predictive maintenance can still be applied to cycloidal reducers.

The rotational frequencies of bearings and toothed gear sets are common items monitored by predictive maintenance practitioners. Bearing rotational frequencies can be obtained from bearing suppliers or calculated, given the relevant system information. Frequencies suggested for monitoring are 1 × shaft rpm for inner race faults and 1 × FTF (fundamental train frequency) for rolling element faults (2).

A cycloidal eccentric bearing presents an uncommon case since both bearing races rotate. Cycloidal discs mesh with pins or rollers located along the inner perimeter of the ring gear housing. As the discs and the pins (or rollers) mesh, a contact frequency is created which can be monitored. See figures 2 – 4. The user can calculate the cycloidal disc mesh frequency by using:

$$\textbf{Cycloidal Disc Mesh Frequency} \sim DMF = \frac{No.\ of\ Pins \times Output\ RPM}{60}\ \text{Hz}$$

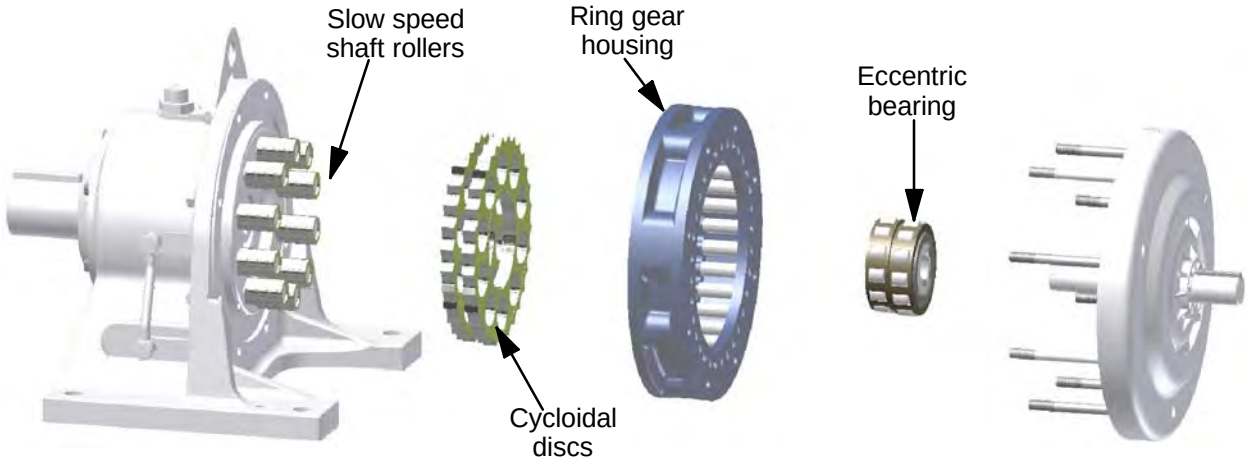

Figure 1. Exploded view of cycloidal reduction components

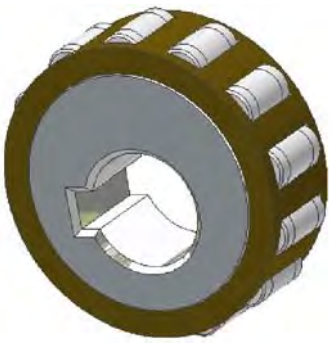

Figure 2. Cycloidal eccentric bearing

Figure 3. Cycloidal disc

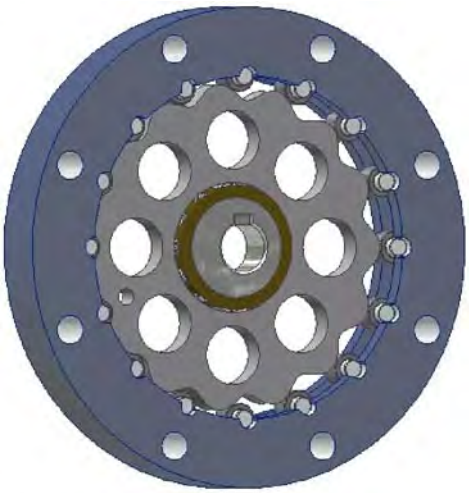

Figure 4. Cycloidal disc meshes with pins or rollers

Predictive maintenance procedure

The key to successful predictive maintenance programs for cycloidal reducers and gearmotors is to record a baseline of a cycloidal unit's vibration frequencies for use a reference as soon as possible after a unit is placed into service. As long as the unit is installed securely, aligned correctly, and its operating loads and conditions match those used for the unit selection, the resulting baseline will be accurate.

A predictive maintenance program for cycloidal speed reducers and gearmotors utilizing vibration analysis is implemented as follows:

1. Install the unit according to the manufacturer's instructions, making sure the unit is mounted securely and aligned correctly. A poor installation will result in an inaccurate baseline.
2. Run the unit under nominal application conditions until it reaches operating temperature.
3. Record a vibration measurement, and note the amplitudes of the eccentric cam and the eccentric bearing fundamental train frequencies.
4. Store this measurement record for future reference. This is the baseline against which all future measurements should be compared.
5. Periodically record a vibration measurement and compare it against the baseline, checking for vibration amplitude increases. The measurement interval will depend on a unit's operating loads and conditions. It's recommended to record measurements frequently at the beginning of a predictive maintenance program, and then adjust the interval according to the unit's maintenance requirements (3).
6. When vibration amplitude increases are noted at the eccentric cam or the eccentric bearing fundamental train frequencies, eccentric bearing wear may have begun. Decrease the vibration measurement interval in order to compare the unit's condition to its baseline more often.
7. Once vibration amplitude increases are noted at higher frequencies, schedule the unit for repair. Advanced wear has most likely begun, so the unit should be removed from service in order to replace worn internal components before catastrophic failure occurs.

Test procedure

A cycloidal reducer was returned which had suffered the typical damage associated with overload or inadequate lubrication: a worn eccentric bearing, pressure marks in the surface of the cycloidal discs' center holes, and burned grease. With the exception of burned grease, this damage also

occurs at the end of a properly selected unit's useful life. Therefore, it was selected as the subject for this study. The unit's eccentric bearing FTF was calculated to be 11.20 Hz, and its cam frequency was determined to be 29.17 Hz. The cycloidal DMF was calculated as 14.75 Hz.

A new, identical unit was assembled in order to obtain a baseline measurement. After obtaining the baseline with a vibration data collector as shown in figure 5, the new unit's eccentric bearing, cycloidal discs, and ring gear assembly were exchanged for those from the damaged unit in a progressive manner in order to simulate the progression of typical wear. If a unit's eccentric bearing becomes worn and the unit continues to operate, wear progresses to the cycloidal discs. Further operation leads to wear within the ring gear assembly. The wear's progression is due to the flow of metallic particles between the internal components by way of the lubricant.

During the last phase, the worn components were installed in the new unit individually in an attempt to isolate the operating frequencies characteristic of those components. The ring gear assembly frequencies were of particular interest, for they are difficult to calculate.

Testing Procedure

All tests were conducted under full load.

1. The returned unit was measured with a vibration analyzer. This provided the data for the total failure condition.
2. A new unit identical to the returned unit was assembled.
3. The new unit was measured with the vibration analyzer to record a baseline.
4. The new unit's eccentric bearing was exchanged for the returned unit's worn eccentric bearing, and the vibrations of the new unit were measured. This provided data for the failure mode of eccentric bearing damage.
5. Keeping the worn eccentric bearing in the new unit, the unit's cycloidal discs were exchanged for the returned unit's discs. The vibrations of the new unit having the worn eccentric bearing and cycloidal discs were measured to obtain data showing the next stage of wear.

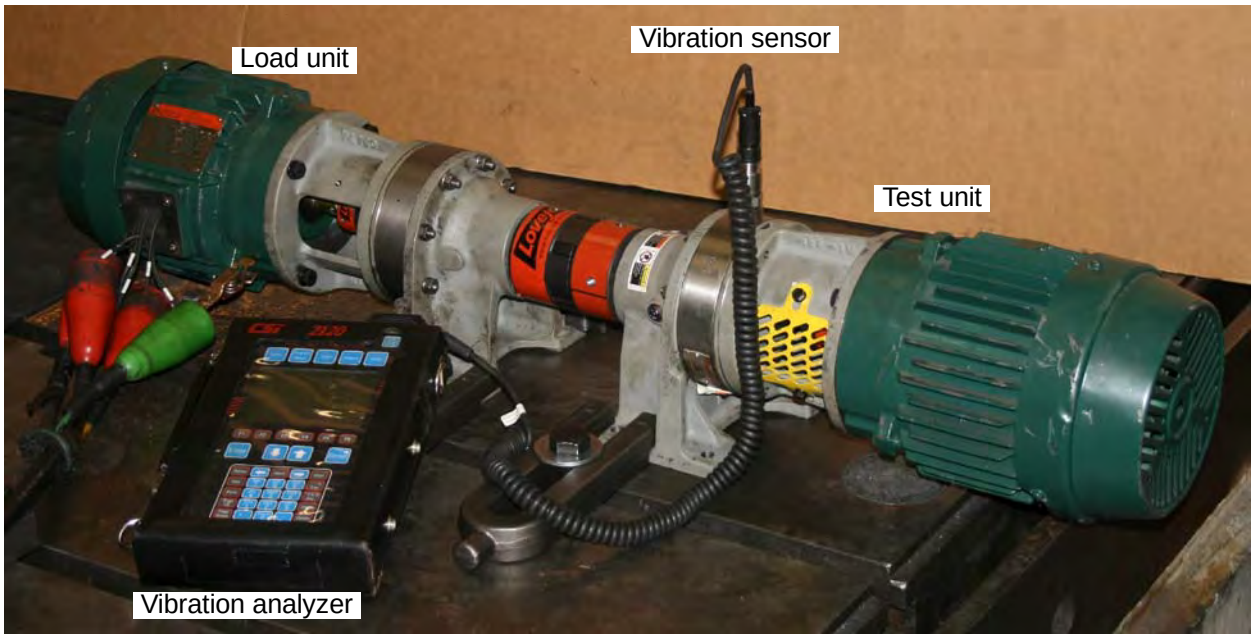

Figure 5. Vibration measurement set-up

6. With the worn eccentric bearing and discs in the new unit, the returned unit's ring gear assembly was installed, see figure 6. The new unit's vibrations were measured to obtain data showing the final level of progressive cycloidal failure – eccentric bearing failure combined with disc and ring gear assembly damage.

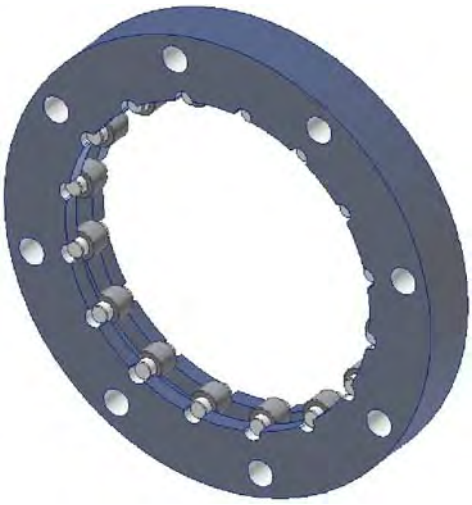

Figure 6. Cycloidal ring gear assembly

7. The new eccentric bearing and ring gear assembly were returned to the new unit. With the worn cycloidal discs still in the new unit, the new unit's vibrations were measured to obtain data showing how cycloidal disc wear contributes to the vibration graph.

8. The cycloidal discs and ring gear assemblies were exchanged between the units, so that the new unit had the new eccentric bearing, the new cycloidal discs, and the worn ring gear assembly. The new unit was measured to obtain data showing how ring gear assembly wear contributes to the vibration graph.

The load and test units were identical, and the input motors operated at a 1750 rpm input speed. A CSI (Computational Systems Incorporated) 2120 single channel machinery analyzer, model A212001, was used to measure the test unit's vibration. The analyzer's parameters were established as shown in figure 7.

The vibration measurements were documented using CSI's MasterTrend RBMWare version 4.60, dated September 4, 2001.

```
                VIEW PERIODIC ANALYSIS PARAMETER SET INFORMATION

Set 1                                          Number of Parameters -  6

FFT:  0.0 - 1000.0 Hz
LOW FREQUENCY CUT-OFF:  2.0 Hz

LINES/AVERAGES       :  1600/6
AVERAGING MODE       :  Normal
WINDOW TYPE          :  Hanning
SPECTRAL WEIGHTING   :  None
THIRD-OCTAVE ANALYSIS:  No

SST CONTROL          :  No
PRE-CONDITIONING UNIT :  Disabled
  FILTER SETTING     :  None
  PEAK ANALYSIS METHOD:  None

SPECIAL TIME WAVEFORM:  No
  FMAX               :  10.50 Hz
  DATA UNITS         :  Default
  NUMBER OF POINTS   :  1024
  TRIGGER            :  None
```

Figure 7. Vibration analyzer measurement parameters

Results

It's important to note that the cycloidal operating frequencies a customer will see on a vibration graph will depend on a unit's size and speed reduction ratio. The graphs shown in figures 8 – 19 and 25 – 48 are specific to the units we tested. The operating frequencies we measured are not applicable to all cycloidal reducers.

Figures 8 – 13 show the vibration graphs a customer might see if the customer were to measure a worn cycloidal reducer. Figure 6 reveals some activity.

An evaluation of the vibrations in more detail, however, reveals areas of concern. In figure 10 we see the acceleration frequencies. The presence of peaks at the higher frequencies indicates there may be roller bearing problems. Sidebands accompanying these peaks are another indication. At this point, the operating frequencies of the eccentric bearing should be examined.

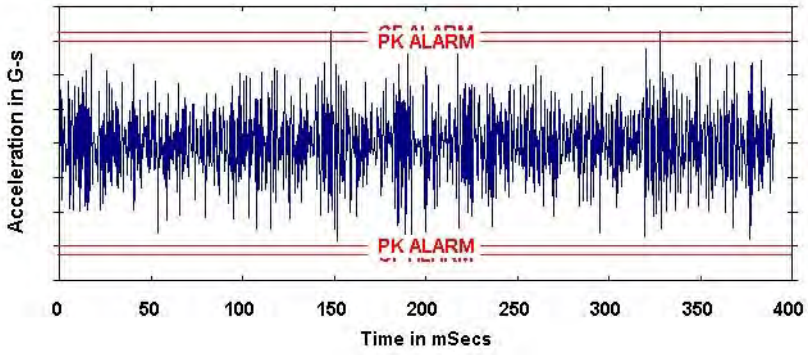

Figure 8. Waveform – returned unit

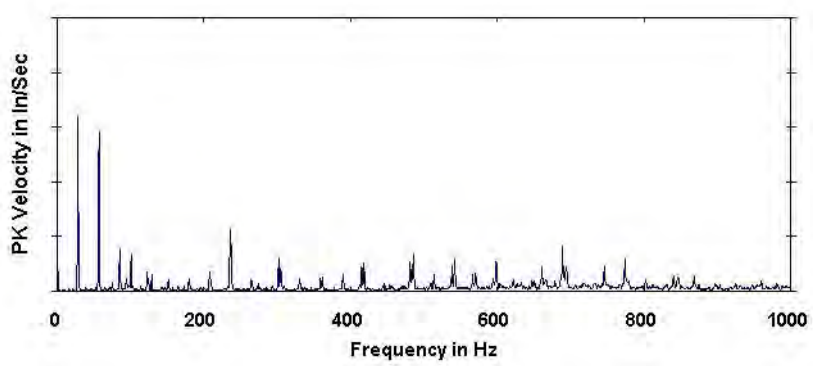

Figure 9. Velocity frequency graph – returned unit

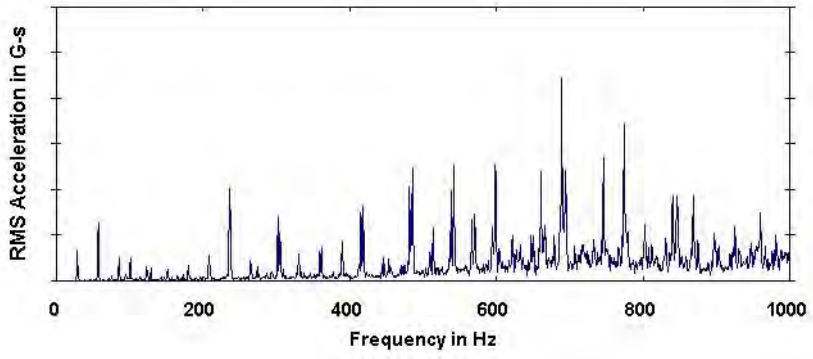

Figure 10. Acceleration frequency graph – returned unit

The velocity frequencies were accessed with the vibration analysis software and the cursor was placed around 29 Hz, the eccentric bearing cam frequency. Figure 11 shows the result. The peak velocity occurs at that frequency, and it's second harmonic is not much less.

The cursor was next placed around 11.20 Hz, the eccentric bearing's FTF, to check for eccentric bearing roller faults. Many harmonics were discovered, with the higher ones having sidebands. See figure 12 below.

Finally, the cycloidal disc mesh frequency of 14.75 Hz was checked. Figure 13 shows that harmonics are present, but their velocity levels are low.

If this unit were located in a noisy environment, it would be difficult to hear its operation. Such an environment would make a baseline reference more valuable. The customer in this case did not detect the progression of wear, so the unit wasn't returned until it failed catastrophically after three months. Let's examine how a baseline measurement would have been useful.

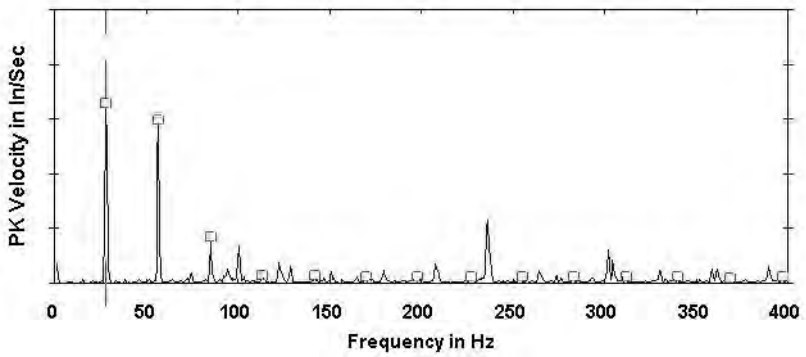

Figure 11. Eccentric bearing cam frequency graph – returned unit

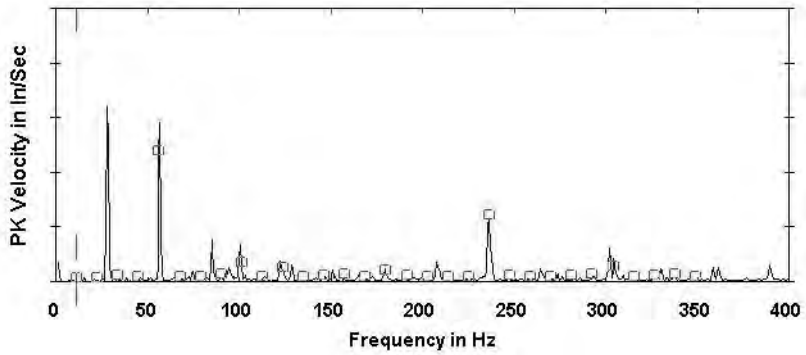

Figure 12. Eccentric bearing rollers frequency graph – returned unit

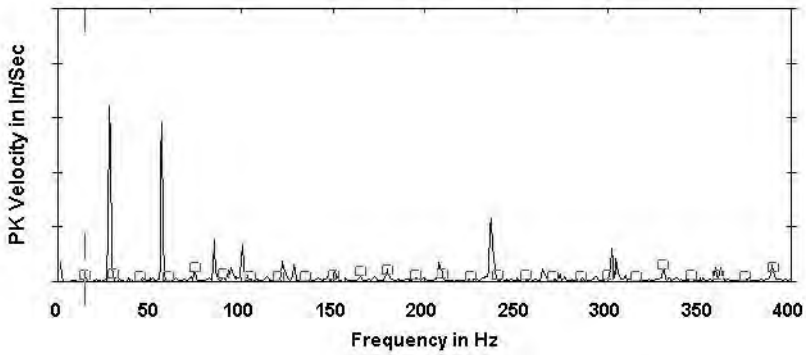

Figure 13. Cycloidal disc mesh frequency graph – returned unit

Figures 14 – 19 show a baseline recorded from the new unit. If customers record such a baseline immediately after installing a unit, then future measurements can be compared to it so that wear can be detected before catastrophic failure occurs. This is especially useful in noisy environments, where machine component noise can be difficult to differentiate.

Each figure has a corresponding one among figures 8 – 13. The comparison of figure 14 with figure 8 shows that the returned unit creates much higher acceleration values than the new one. Clearly, something in the returned unit has changed. Figure 15 vs. figure 9 and figure 16 vs. figure 10 reveal amplitude increases and sidebands at the higher frequencies. These changes suggest defective elements among the cycloidal reduction components. The same effects are noted when the components are evaluated by comparing figures 17 – 19 against figures 11 – 13. These observations signal that some amount of wear has occurred to all of them.

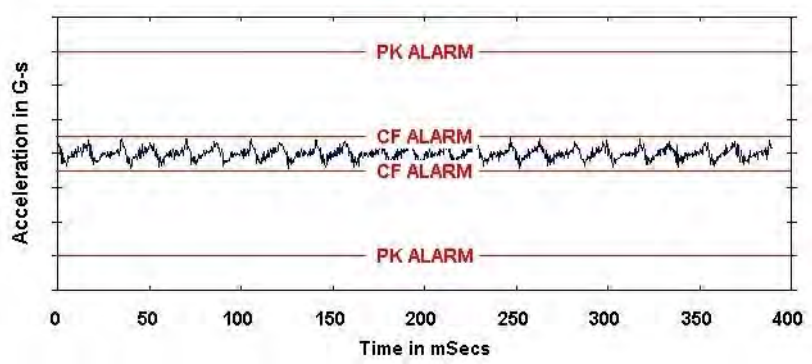

Figure 14. Waveform – new unit

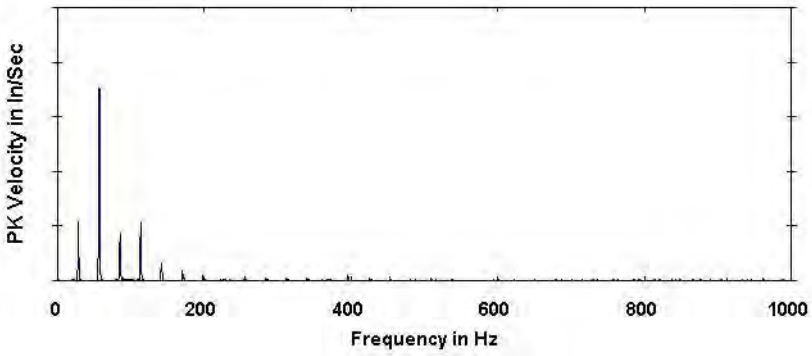

Figure 15. Velocity frequency graph – new unit

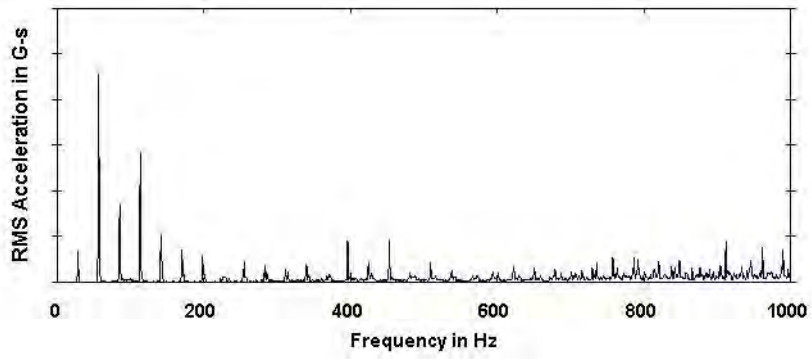

Figure 16. Acceleration frequency graph – new unit

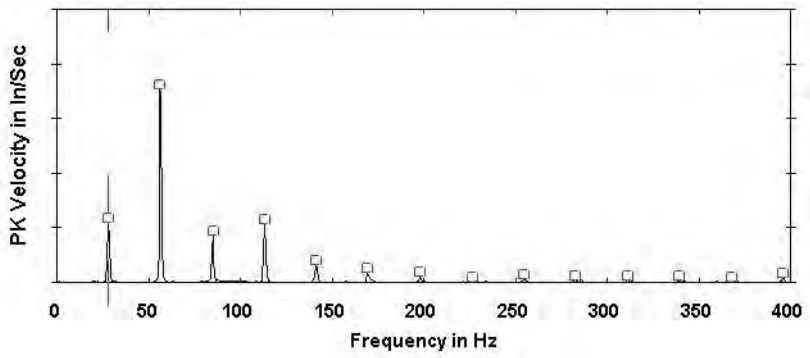

Figure 17. Eccentric bearing cam frequency graph – new unit

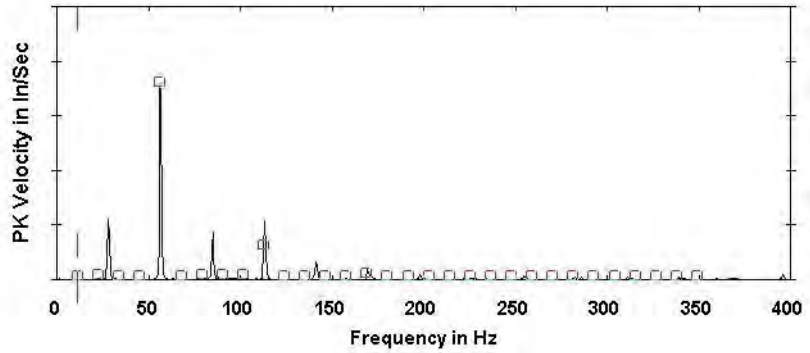

Figure 18. Eccentric bearing rollers frequency graph – new unit

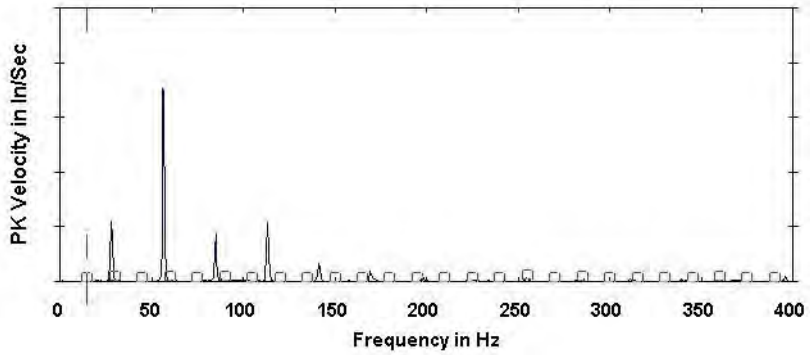

Figure 19. Cycloidal disc mesh frequency graph – new unit

In an overloaded or inadequately lubricated condition, the reducer will overheat. Undetected, the overheating causes lubrication failure and discoloration of the bearing elements. Pitting, which progresses to flaking and sometimes spalling, results shortly thereafter. Figure 20 shows the appearance of the worn eccentric bearing that was removed from the returned unit.

Once flakes from the eccentric bearing are free to flow between the components via the lubricant, the flakes will create indentations in the contact surfaces of the cycloidal disc center holes. The returned unit suffered such damage, as shown in figure 21. Additionally, the ring gear assembly components will suffer wear. Figures 22 – 24 illustrate the Micropitting and abrasion that occurred to the returned unit's components.

As described in steps 4 – 6 of the testing procedure, the worn components were substituted into the new unit in a manner that follows the progression of internal wear. Figures 25 – 30 were obtained after the new unit's eccentric bearing was replaced with the worn unit's eccentric bearing. Increases in all of the frequency amplitudes are noticeable.

a) Eccentric bearing rollers

b) Eccentric bearing cam

Figure 20. Eccentric bearing damage due to overload or inadequate lubrication

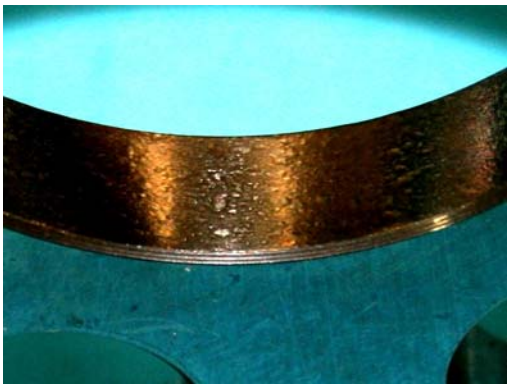

Figure 21. Indentations in a cycloidal disc center hole

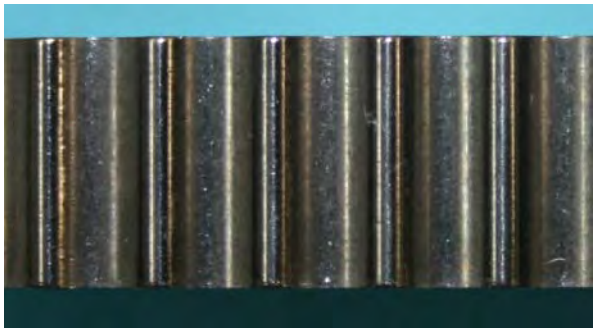

Figure 22. Micropitting of the cycloidal disc lobes

Figure 23. Micropitting of the ring gear pins

Figure 24. Mild abrasion in the ring gear pin bores

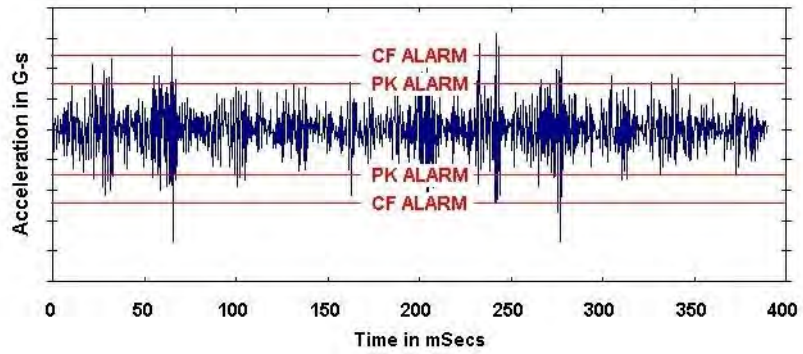

Figure 25. Waveform – new unit with the worn eccentric bearing; see figures 8 and 14 for comparison

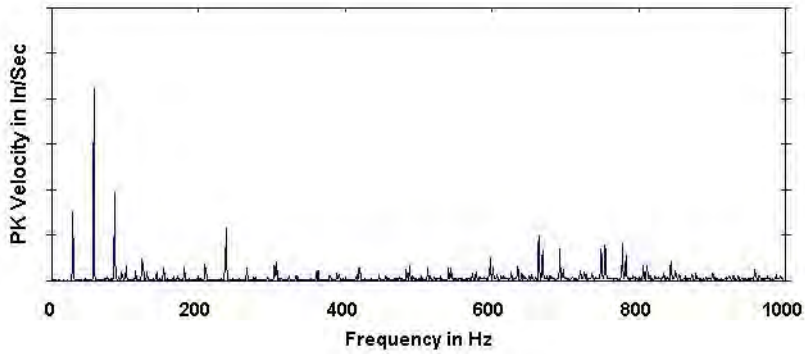

Figure 26. Velocity frequency graph – new unit with the worn eccentric bearing; see figures 9 and 15 for comparison

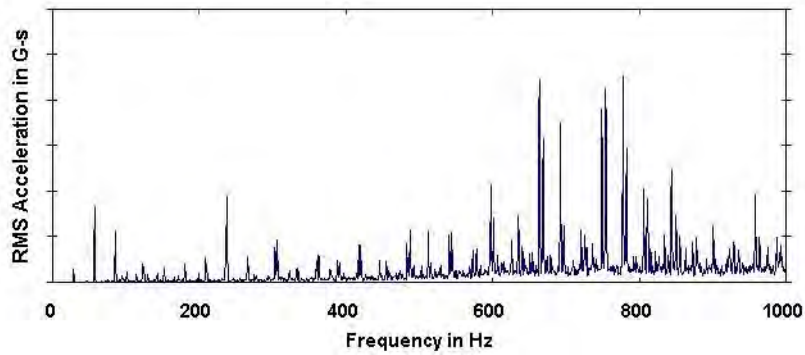

Figure 27. Acceleration frequency graph – new unit with the worn eccentric bearing; see figures 10 and 16 for comparison

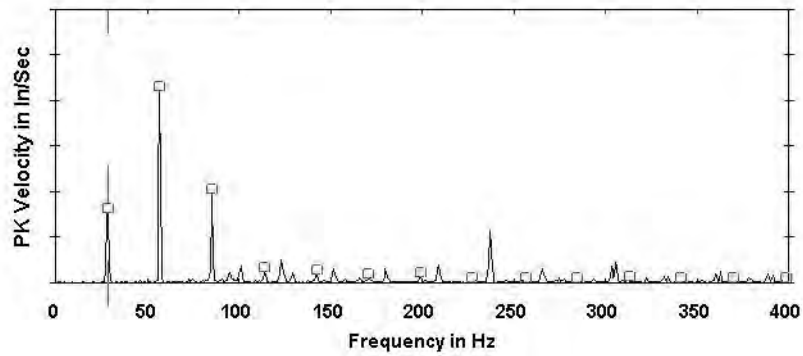

Figure 28. Eccentric bearing cam frequency graph – new unit with the worn eccentric bearing; see figures 11 and 17 for comparison

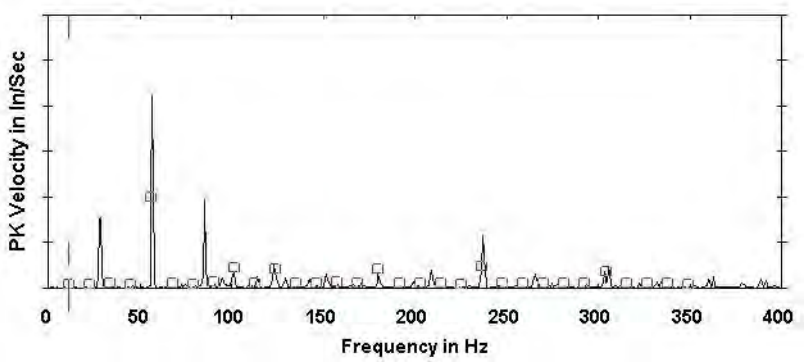

Figure 29. Eccentric bearing rollers frequency graph – new unit with the worn eccentric bearing; see figures 12 and 18 for comparison

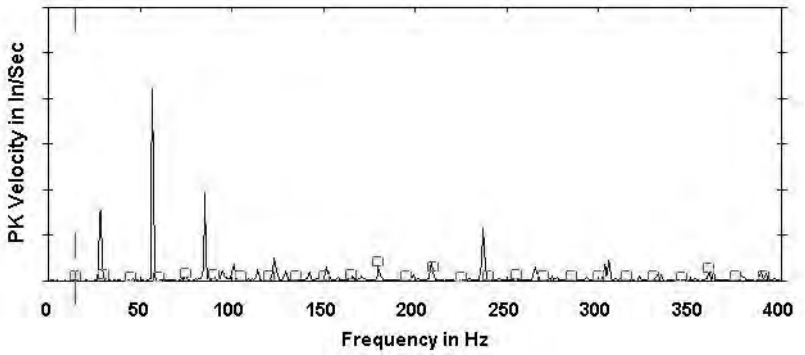

Figure 30. Cycloidal disc mesh frequency graph – new unit with the worn eccentric bearing; see figures 13 and 19 for comparison

Next, the new unit was opened and the new discs were exchanged for the discs from the worn unit. The subsequent measurements are provided in figures 31 – 36. Note that frequency amplitudes increased above those in figures 25 – 30, but the increases weren't as dramatic as those created by the eccentric bearing alone. Figures 8 – 13 represent the final stage in the wear progression, which includes the ring gear assembly. They are very similar to figures 31 – 36. Due to their similarity, procedures 9 and 10 were performed in order to determine what contributions the cycloidal discs and the ring gear assembly made to the vibration measurements.

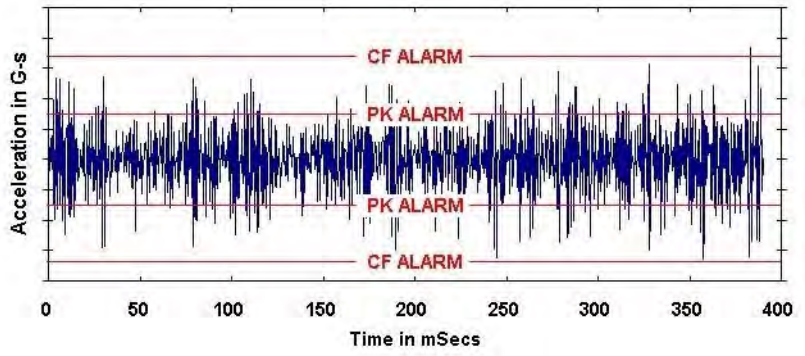

Figure 31. Waveform – new unit with the worn eccentric bearing and worn cycloidal discs; see figure 25 for comparison

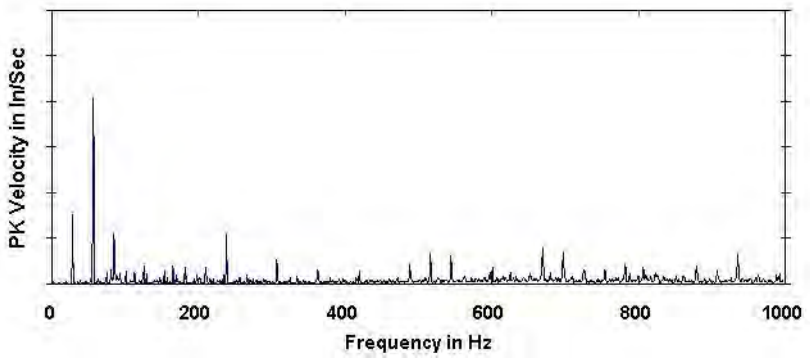

Figure 32. Velocity frequency graph – new unit with the worn eccentric bearing and worn cycloidal discs; see figure 26 for comparison

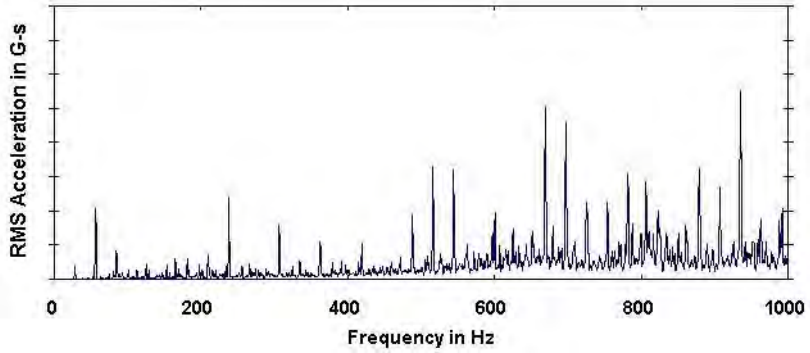

Figure 33. Acceleration frequency graph – new unit with the worn eccentric bearing and worn cycloidal discs; see figure 27 for comparison

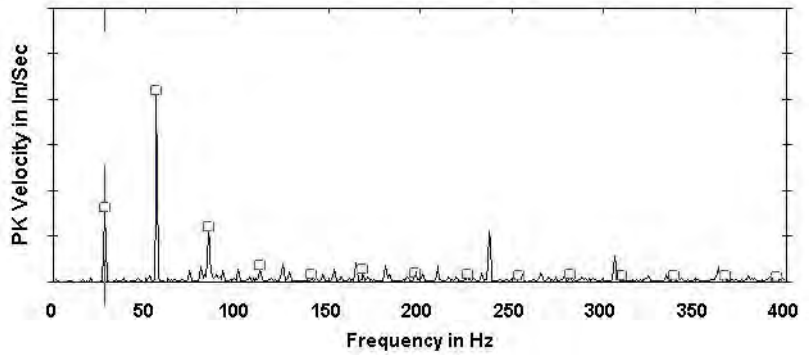

Figure 34. Eccentric bearing cam frequency graph – new unit with the worn eccentric bearing and worn cycloidal discs; see figure 28 for comparison

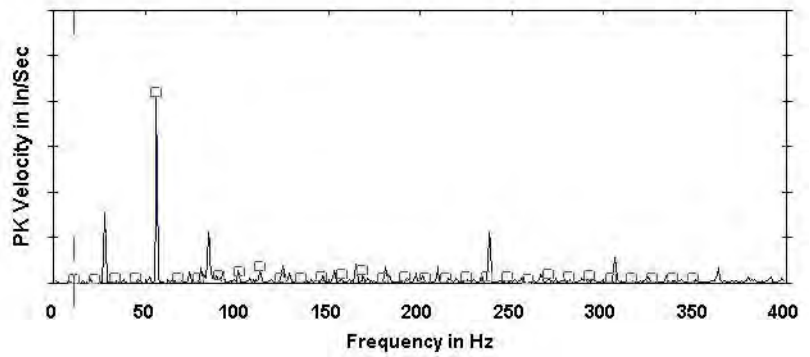

Figure 35. Eccentric bearing rollers frequency graph – new unit with the worn eccentric bearing and worn cycloidal discs; see figure 29 for comparison

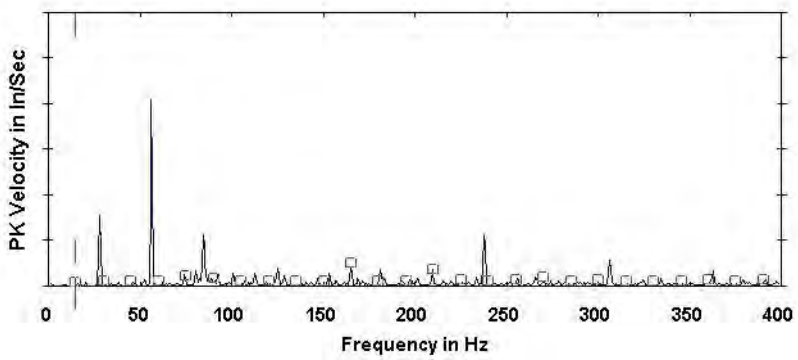

Figure 36. Cycloidal disc mesh frequency graph – new unit with the worn eccentric bearing and worn cycloidal discs; see figure 30 for comparison

The new eccentric bearing was returned to the new unit while the worn cycloidal discs remained installed, according to step 9. The results are presented in figures 37 – 42. Additional disturbance can be seen in the waveform when figure 37 is compared to figure 14, but the waveform that was presented after the unit was newly assembled (all new components) is still recognizable. A comparison of the corresponding acceleration frequency graphs, figure 39 vs. figure 16, reveals minor amplitude increases at the higher frequencies. There are no discernable amplitude increases in any of the velocity frequency graphs. For example, figures 41 and 42 are indistinguishable from figures 18 and 19, respectively.

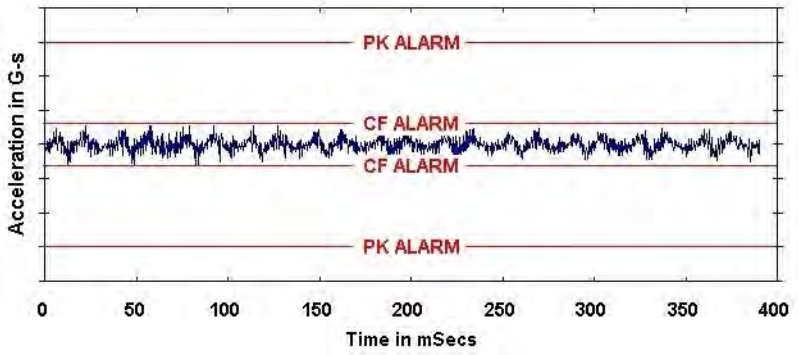

Figure 37. Waveform – new unit with the worn cycloidal discs; see figure 14 for comparison

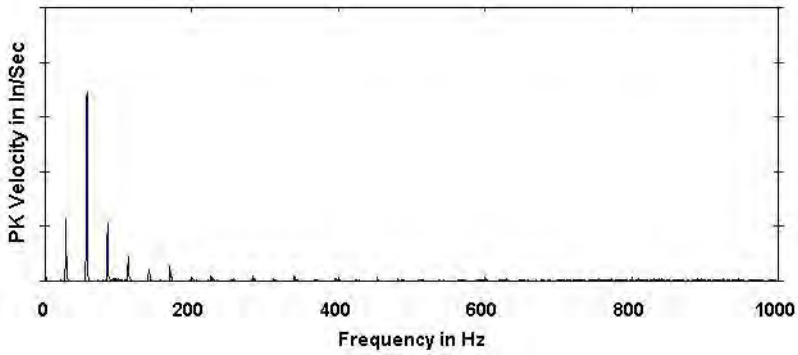

Figure 38. Velocity frequency graph – new unit with the worn cycloidal discs; see figure 15 for comparison

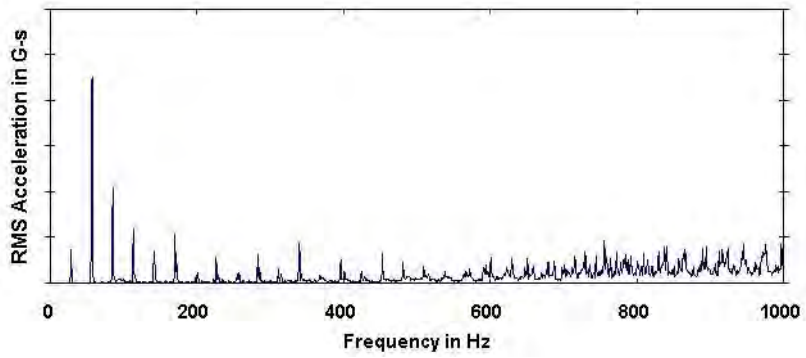

Figure 39. Acceleration frequency graph – new unit with the worn cycloidal discs; see figure 16 for comparison

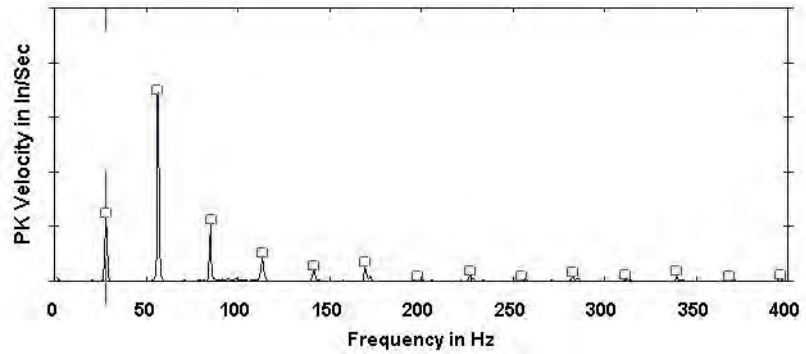

Figure 40. Eccentric bearing cam frequency graph – new unit with the worn cycloidal discs; see figure 17 for comparison

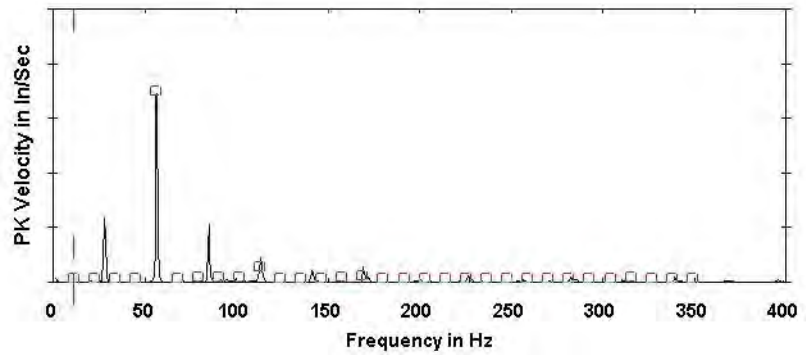

Figure 41. Eccentric bearing rollers frequency graph – new unit with the worn cycloidal discs; see figure 18 for comparison

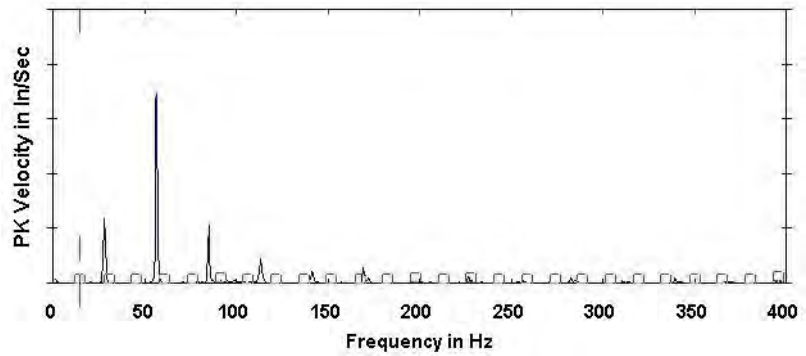

Figure 42. Cycloidal disc gear mesh frequency graph – new unit with the worn cycloidal discs; see figure 19 for comparison

To conclude the tests, the new cycloidal discs were reinstalled in the new unit while its new ring gear assembly was exchanged for the worn one. Figures 43 – 48 show the measurements. A comparison of figure 43 against figure 14 shows a smaller disturbance than in figure 37, and the waveform that was presented after the unit was newly assembled is more recognizable. There is no significant difference between the acceleration frequency graphs in figures 45 and 16. As with the previous component arrangement, there is no noticeable difference in the cycloidal disc mesh frequency amplitudes between the new and worn ring gear assemblies. Refer to figures 48 and 19.

Shortly after completing the initial tests, we received the opportunity to analyze a unit having worn cycloidal discs but a good eccentric bearing. In this case, the wear resulted from lubrication failure. Figures 49 – 52 show the worn components, and figures 53 – 76 illustrate the vibration measurement results.

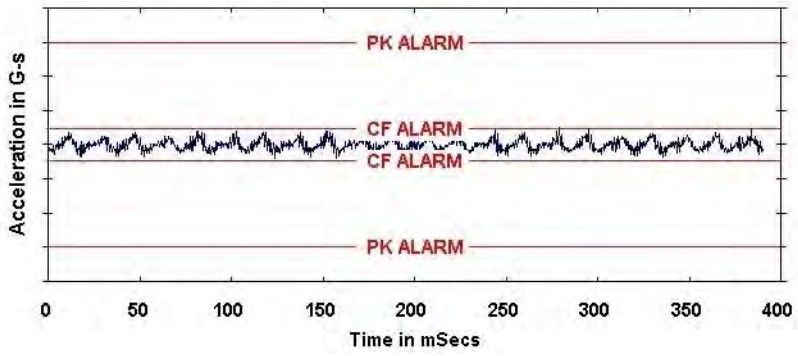

Figure 43. Waveform – new unit with the bad ring gear assembly; see figure 14 for comparison

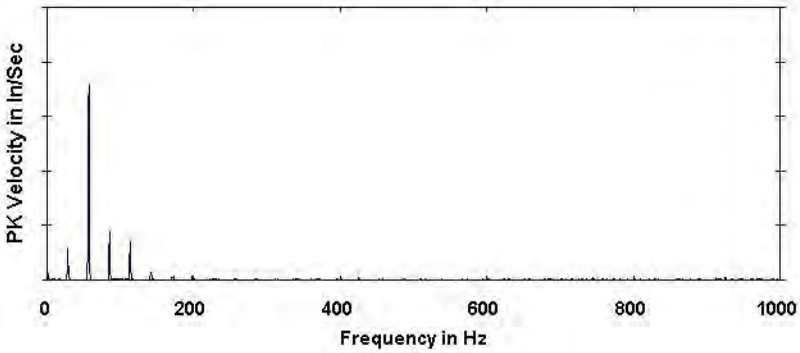

Figure 44. Velocity frequency graph – new unit with the worn ring gear assembly; see figure 15 for comparison

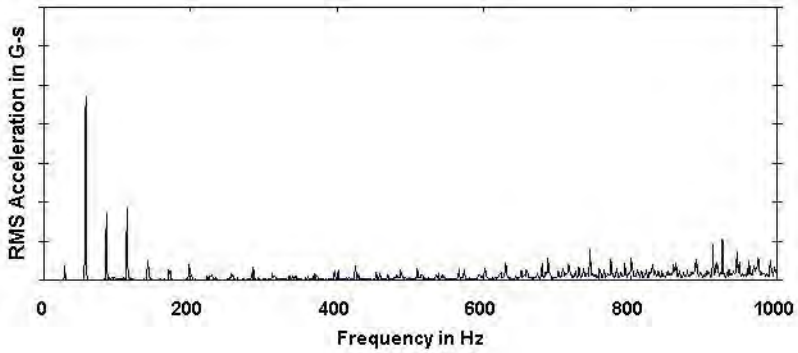

Figure 45. Acceleration frequency graph – new unit with the worn ring gear assembly; see figure 16 for comparison

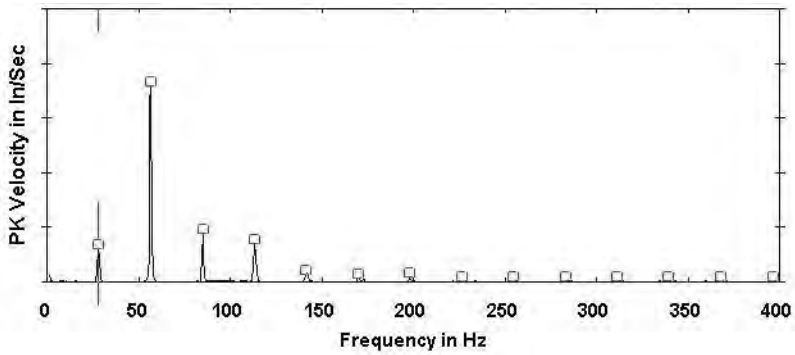

Figure 46. Eccentric bearing cam frequency graph – new unit with the worn ring gear assembly; see figure 17 for comparison

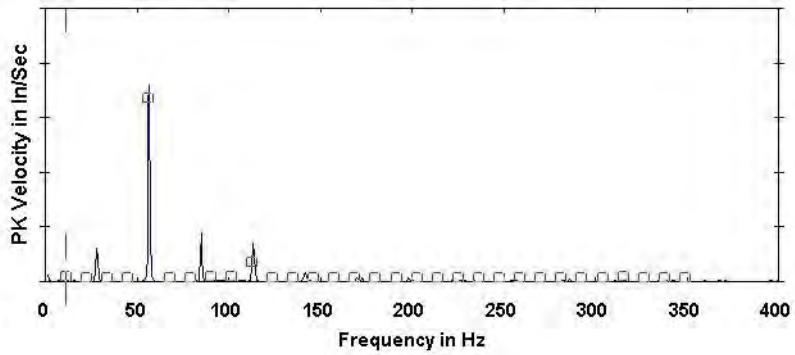

Figure 47. Eccentric bearing roller frequency graph – new unit with the worn ring gear assembly; see figure 18 for comparison

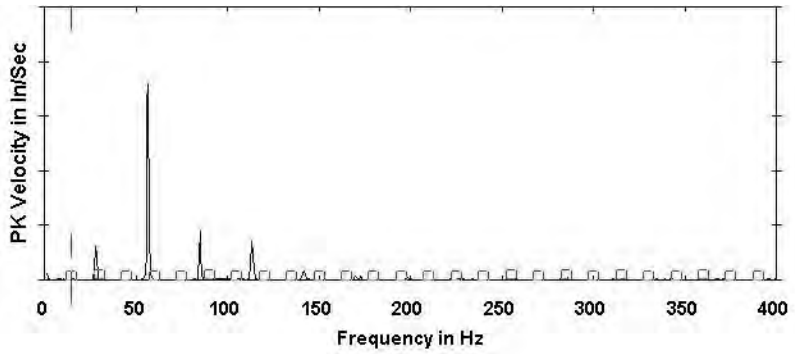

Figure 48. Cycloidal disc mesh frequency graph – new unit with the worn ring gear assembly; see figure 19 for comparison

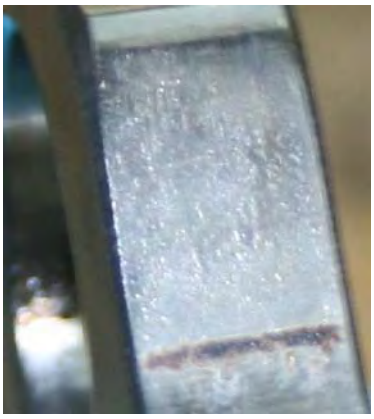

Figure 49. A micropitted disc

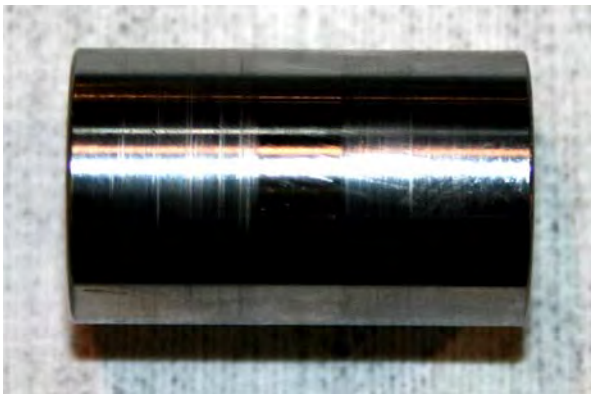

Figure 50. A mildly scuffed slow speed roller

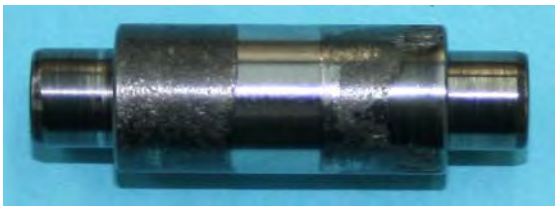

Figure 51. A pitted ring gear roller on its pin

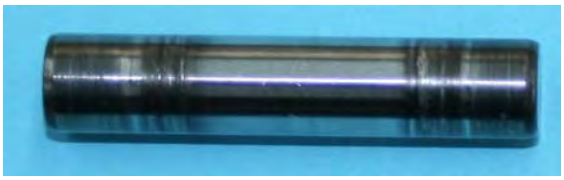

Figure 52. A pitted ring gear pin

Comparisons of the waveform data shown in figures 53, 57, 61, 65, 69 and 73 and the velocity frequency graphs provided in figures 54, 58, 62, 66, 70, and 74 do not reveal anything is obviously amiss with the worn unit. The acceleration frequency graphs displayed in figures 55, 59, 63, 67, 71, and 75, however, highlight the effects of the wear. The wear has induced amplitude increases between 400 – 1000 Hz. Installation of the worn components in the good unit demonstrates that the worn ring gear components lead to the amplitude increases between 400 – 800 Hz, while the worn cycloidal discs and slow speed rollers affected the amplitudes between 800 – 1000 Hz. The red lines in figures 56, 60, 64, 68, 72, and 76 illustrate that the wear had no influence on the cycloidal disc mesh frequency amplitudes.

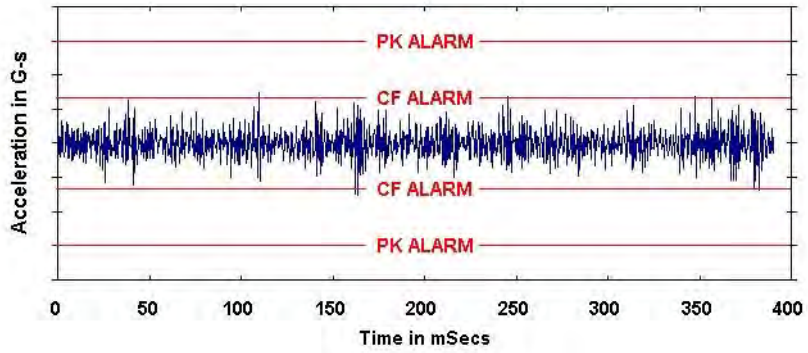

Figure 53. Waveform – test unit with bad cycloidal discs

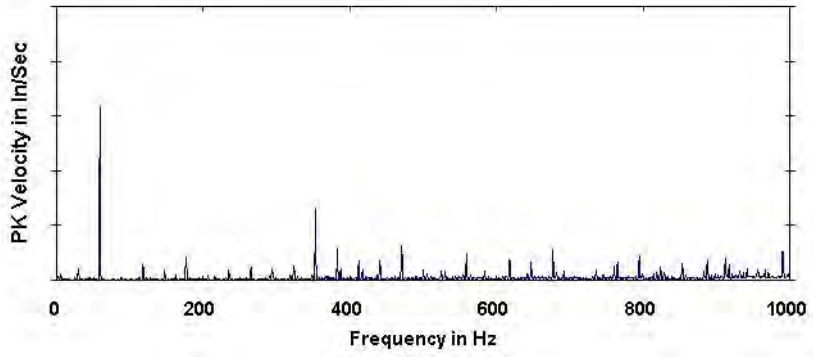

Figure 54. Velocity frequency graph – test unit with bad cycloidal discs

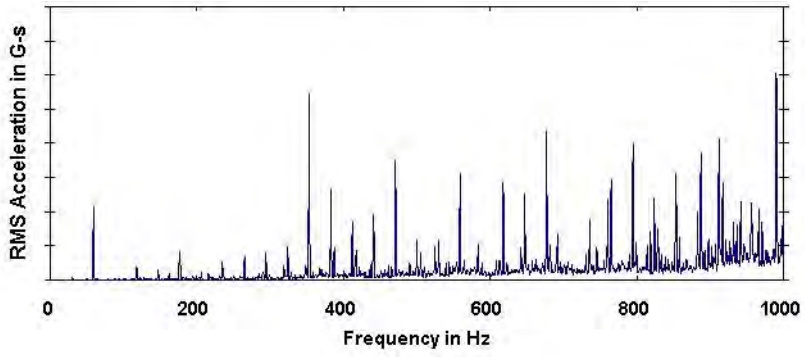

Figure 55. Acceleration frequency graph – test unit with bad cycloidal discs

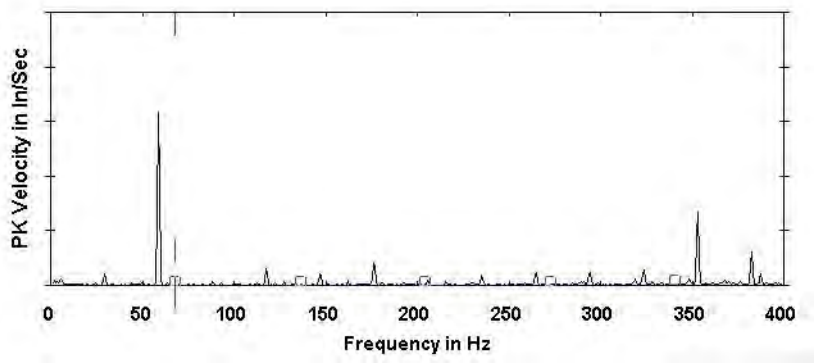

Figure 56. Cycloidal disc mesh frequency graph – test unit with bad cycloidal discs

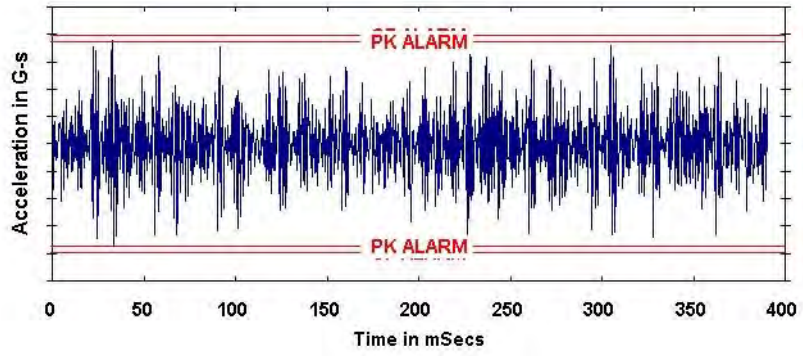

Figure 57. Waveform – good unit

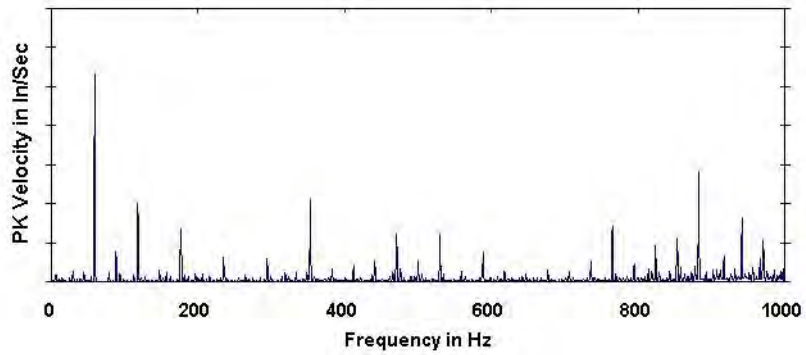

Figure 58. Velocity frequency graph – good unit

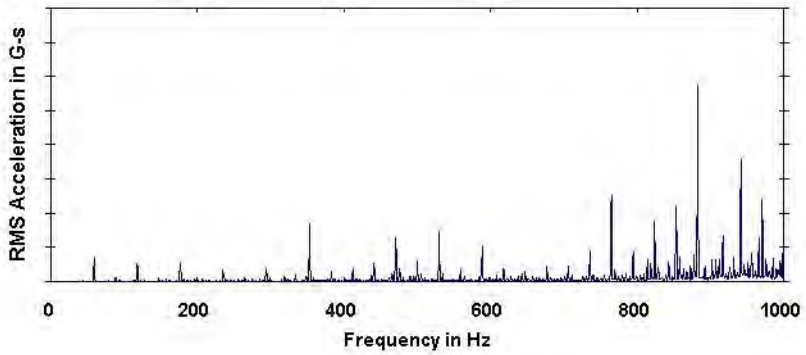

Figure 59. Acceleration frequency graph – good unit

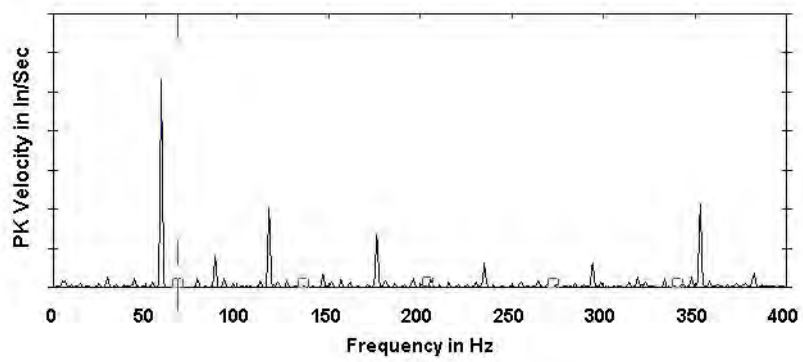

Figure 60. Cycloidal disc mesh frequency graph – good unit

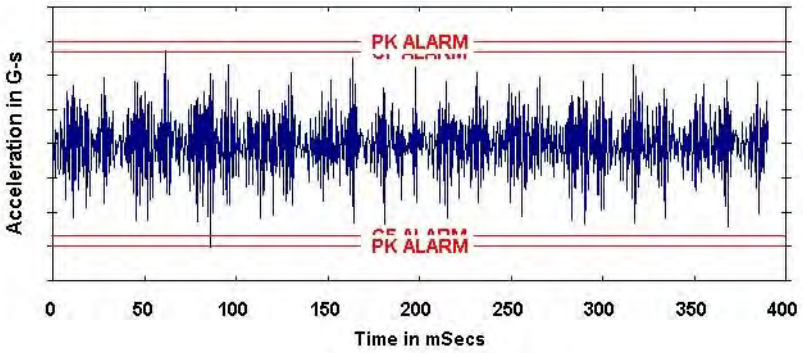

Figure 61. Waveform – good unit with bad cycloidal discs; see figures 53 and 57 for comparison

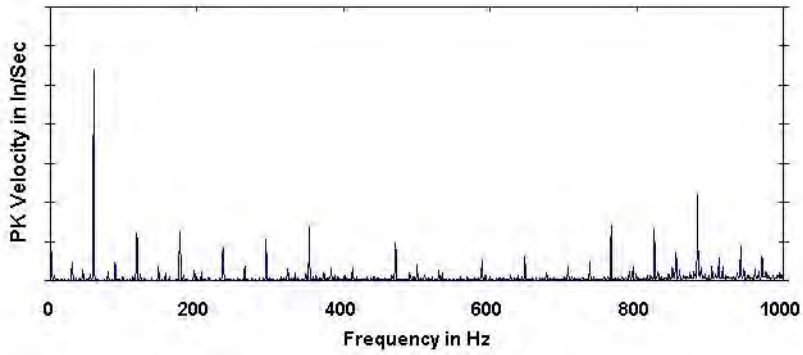

Figure 62. Velocity frequency graph – good unit with bad cycloidal discs; see figures 54 and 58 for comparison

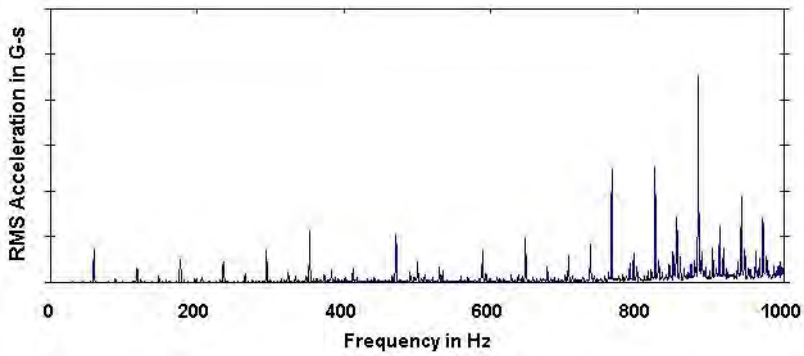

Figure 63. Acceleration frequency graph – good unit with bad cycloidal discs; see figures 55 and 59 for comparison

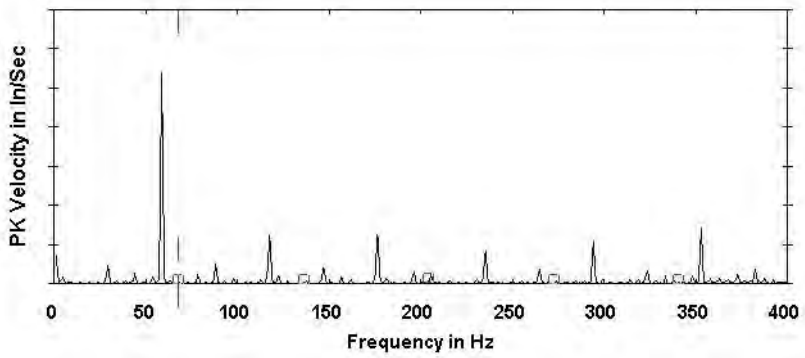

Figure 64. Cycloidal disc mesh frequency graph – good unit with bad cycloidal discs; see figures 56 and 60 for comparison

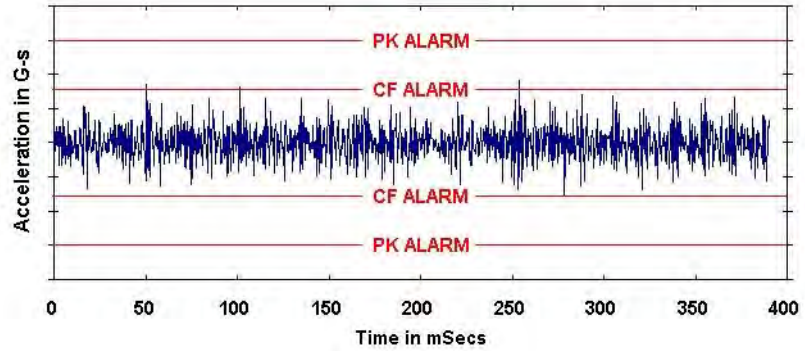

Figure 65. Waveform – good unit with bad ring gear pins; see figure 57 for comparison

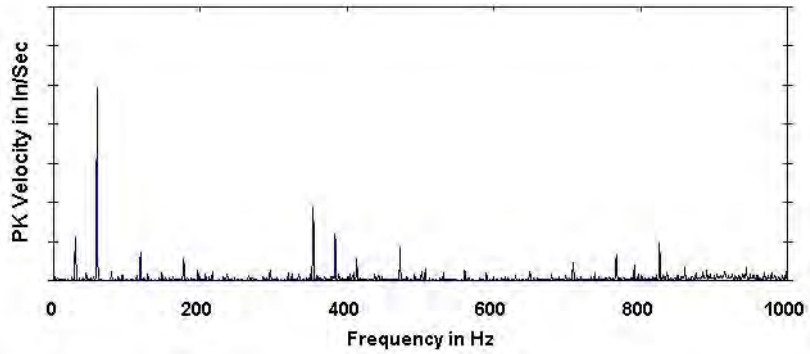

Figure 66. Velocity frequency graph – good unit with bad ring gear pins; see figure 58 for comparison

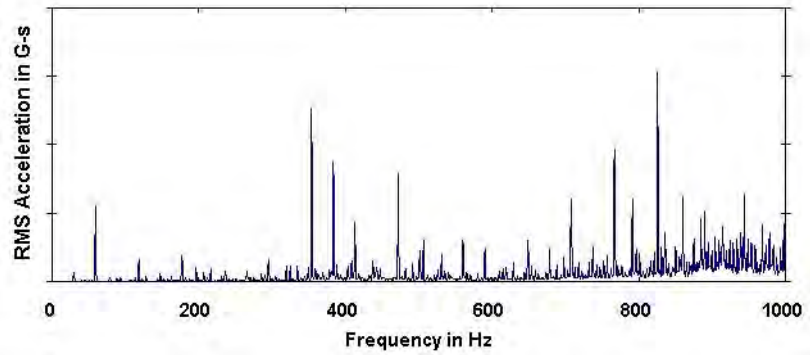

Figure 67. Acceleration frequency graph – good unit with bad ring gear pins; see figure 59 for comparison

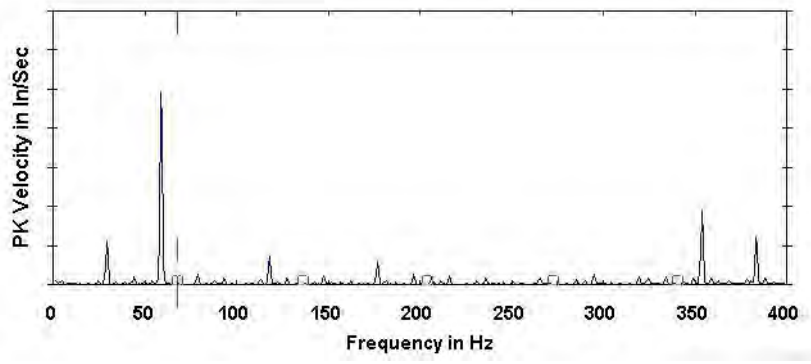

Figure 68. Cycloidal disc mesh frequency graph – good unit with bad ring gear pins; see figure 60 for comparison

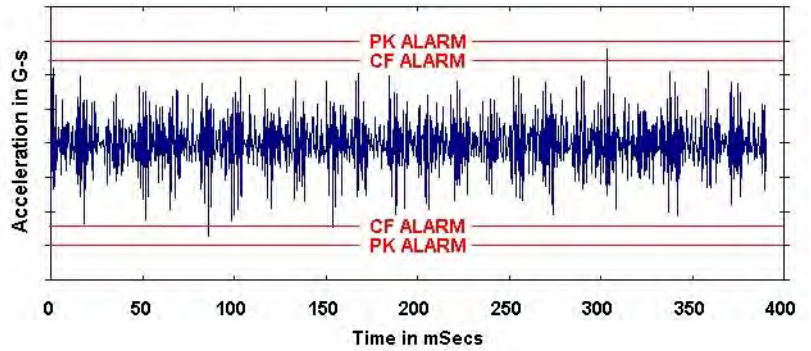

Figure 69. Waveform – good unit with bad ring gear housing; see figure 57 for comparison

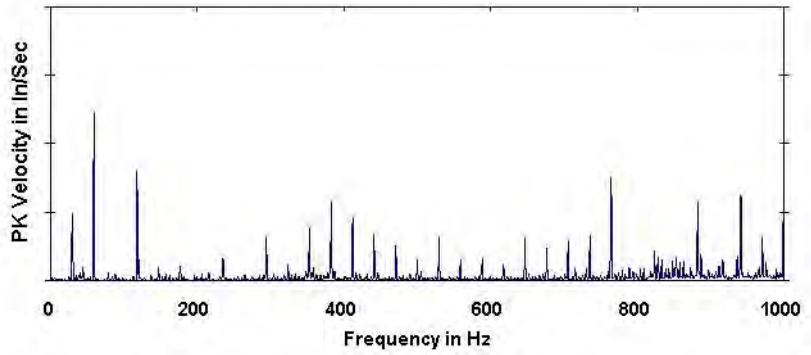

Figure 70. Velocity frequency graph – good unit with bad ring gear housing; see figure 58 for comparison

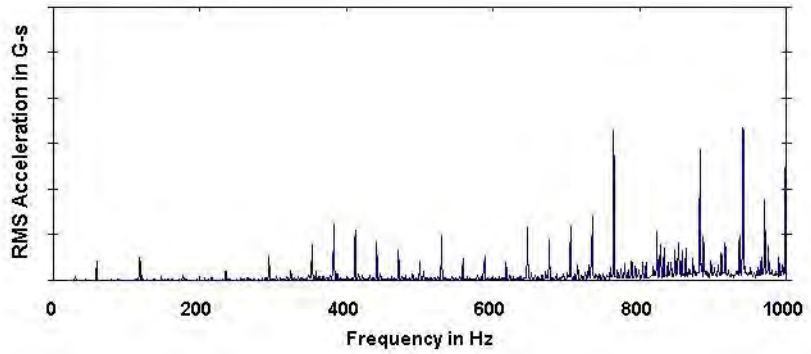

Figure 71. Acceleration frequency graph – good unit with bad ring gear housing; see figure 59 for comparison

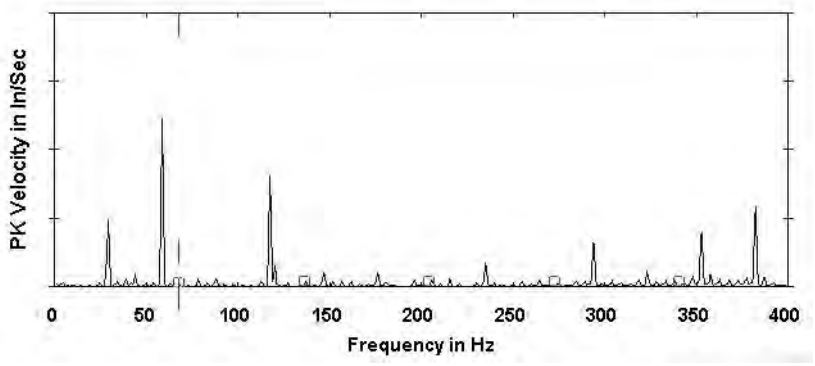

Figure 72. Cycloidal disc mesh frequency graph – good unit with bad ring gear housing; see figure 60 for comparison

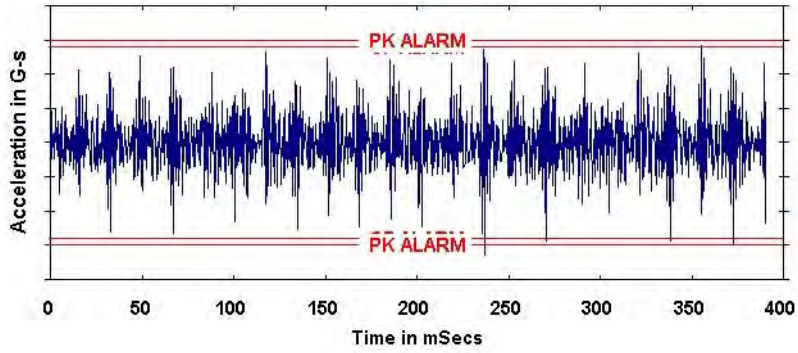

Figure 73. Waveform – Good unit with bad slow speed shaft rollers; see figure 57 for comparison

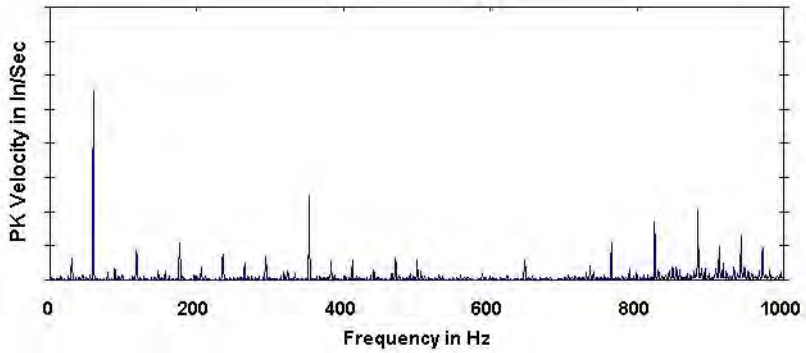

Figure 74. Velocity frequency graph – good unit with bad slow speed shaft rollers; see figure 58 for comparison

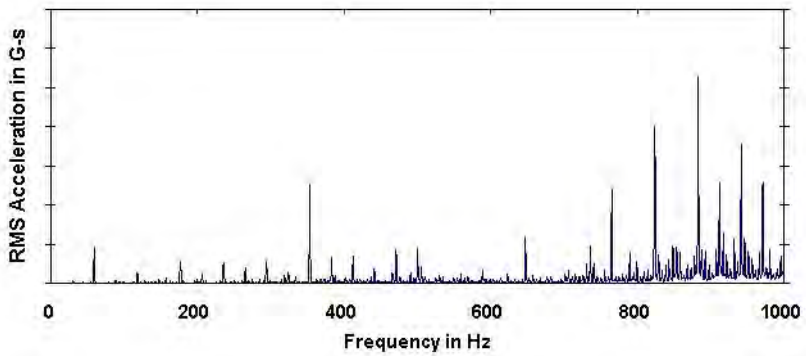

Figure 75. Acceleration frequency graph – good unit with bad slow speed shaft rollers; see figure 59 for comparison

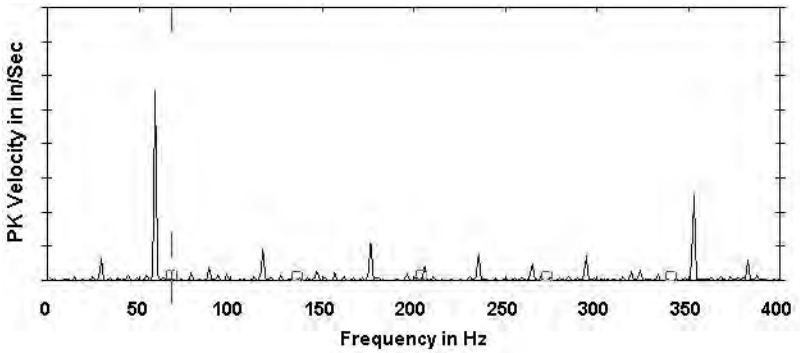

Figure 76. Cycloidal disc mesh frequency – good unit with bad slow speed shaft rollers; see figure 60 for comparison

Conclusion

Since some cycloidal operating frequencies are unknown, it can be difficult to review a single vibration graph and determine which specific internal components are worn. Cycloidal eccentric bearing fundamental train frequencies and disc mesh frequencies can be calculated, however. We also know that rolling element faults may reveal themselves by creating high frequency vibrations that may also include sidebands (2,3).

Wear of the eccentric bearing will begin with pitting. See figure 20b. As the pits become more numerous, an increase in higher frequency amplitudes will be observed when a frequency measurement graph is compared to the reducer's baseline measurement. Sidebands around these higher frequencies will become apparent as well. At this stage of wear, the unit remains operational.

As the wear progresses, pitting of the eccentric bearing rollers will begin. Meanwhile, the pits in the bearing's cam will join and metallic flakes will be released. In order to confirm whether this wear stage has commenced, the eccentric bearing fundamental train frequency should be monitored. Refer to the FTF equation in this paper's introduction and figure 20a for an example of a worn bearing's potential appearance. Additional frequency amplitude increases will be observed upon a baseline comparison at this time in the cycloidal reducer's life cycle. The unit is still operational at this point, but not much life may remain. Hence, reducer repair should be scheduled and the unit should be taken off-line at the next opportunity. Doing so will prevent an unscheduled halt in production, which is one of the predictive maintenance benefits described in the introduction's first paragraph.

If the cycloidal reducer's operation is allowed to continue at this stage of wear, the metallic flakes released by the eccentric bearing will flow between the internal reduction components via the lubricant. Indentations will be created in the cycloidal discs' center holes, as shown in figure 21. Figures 22 and 23 show the micropitting that will be experienced by the cycloidal discs' lobes and the ring gear pins. Figures 37 – 48, however, demonstrate that the wear of these components contributes no significant frequency amplitude increases to the frequency measurement graphs.

This suggests that the cycloidal discs and the ring gear assemblies of properly selected cycloidal reducers, which are subjected to loads no larger and conditions no more severe than those considered during the selection process, will not suffer enough wear damage to appreciably contribute to the vibration increases created by a worn unit. Therefore, a predictive maintenance program's objects of interest among a cycloidal reducer's reduction component set are:

1. The eccentric bearing cam frequency;
2. The eccentric bearing fundamental train frequency.

References

1. Crawford, A. R. and Crawford, S., *The Simplified Handbook of Vibration Analysis Volume 2: Applied Vibration Analysis*, Computational Systems, Inc., p 224, 1992.
2. *Pocket Vibration Troubleshooter's Guide*, CSI Part # A99915 Rev 2, Computational Systems, Inc., p 7, 1995.
3. Crawford, A. R. and Crawford, S., *The Simplified Handbook of Vibration Analysis Volume 2: Applied Vibration Analysis*, Computational Systems, Inc., pp 225, 234, and 236, 1992.